

Introduction

Carbon nanotubes (CNTs) have proved to be very promising fillers for polymer nanocomposites. However, because of the lack of a detailed understanding of the principles of the nano-inclusion interaction with polymer matrixes, the properties of such materials are mostly studied empirically. The properties of polymer chains in contact with a nanoscale filler surface inevitably differ from the properties of a pure polymer. Because of the large area of their effective surface, even at small concentrations of nano-inclusions (on the order of several weight percent), the interfacial area may cover a substantial part of the polymer matrix. The material properties of composite with nanofillers are affected by several parameters: the shape and size of nanoparticles, the distribution of particles in the polymer matrix, the type and force of interaction of the polymer matrix with the nanoparticles, entanglement of polymer chains, etc. In the present study, within the coarse-grained (CG) molecular-dynamics methods, aspects of the interaction of the amorphous polyethylene matrix with carbon nanotubes and graphene nanoparticles. The influence of carbon inclusions on the evolution of polymer matrix during the nanocomposite deformation are studied.

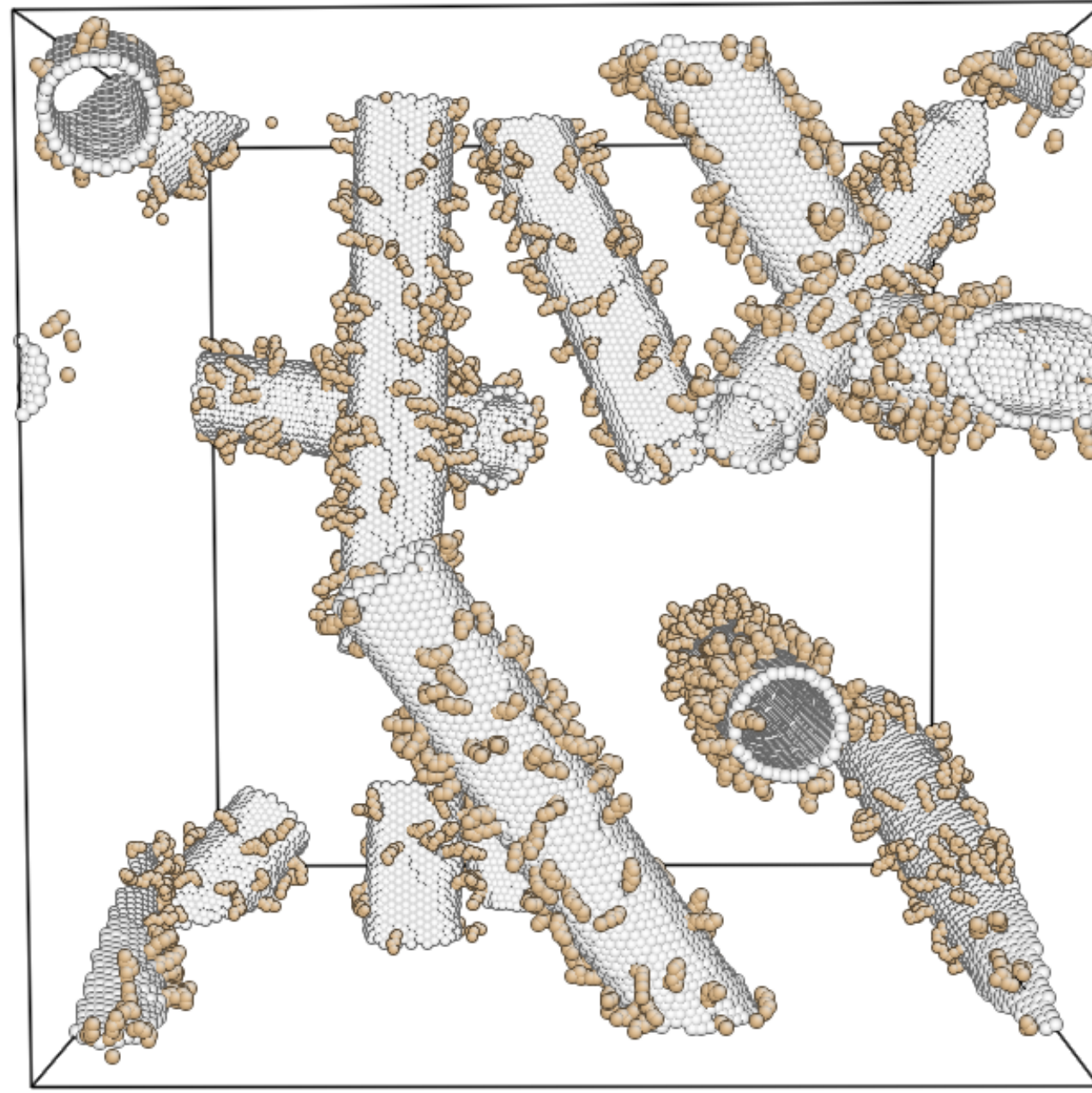


Figure 1. Example of the distribution of nanotubes with a functionalized surface (modified with C₆ groups) in the computational cell.

Model

In order to accelerate calculations, polyethylene was presented in a simplified geometry: CH₂ and CH₃ groups were considered atomic units of the polymer chain (united-atom model). The interatomic interaction in the coarse-grained model was set as:

$$U = U_{\text{bond}} + U_{\text{angle}} + U_{\text{dihedral}} + U_{\text{nonbond}}$$

$$U_{\text{bond}}(r) = \frac{1}{2} k_r (r - r_0)^2$$

$$U_{\text{angle}}(\theta) = \frac{1}{2} k_\theta (\cos \theta - \cos \theta_0)^2$$

$$U_{\text{nonbond}}(r) = 4u \left(\left(\frac{d}{r} \right)^{12} - \left(\frac{d}{r} \right)^6 \right)$$

$$U_{\text{dihedral}}(\phi) = k_\phi (1 + \cos m\phi)$$

The initial topology was obtained with the use of a radical-like polymerization. Chain growth was initiated in a cell initially containing only monomers and a set of CNTs (if needed).



Figure 2. The scheme of the polymer matrix preparation using "radical-like" polymerization (M. Perez et al. J. Chem. Phys. 128, 234904 (2008))

Pure polyethylene uniaxial deformation

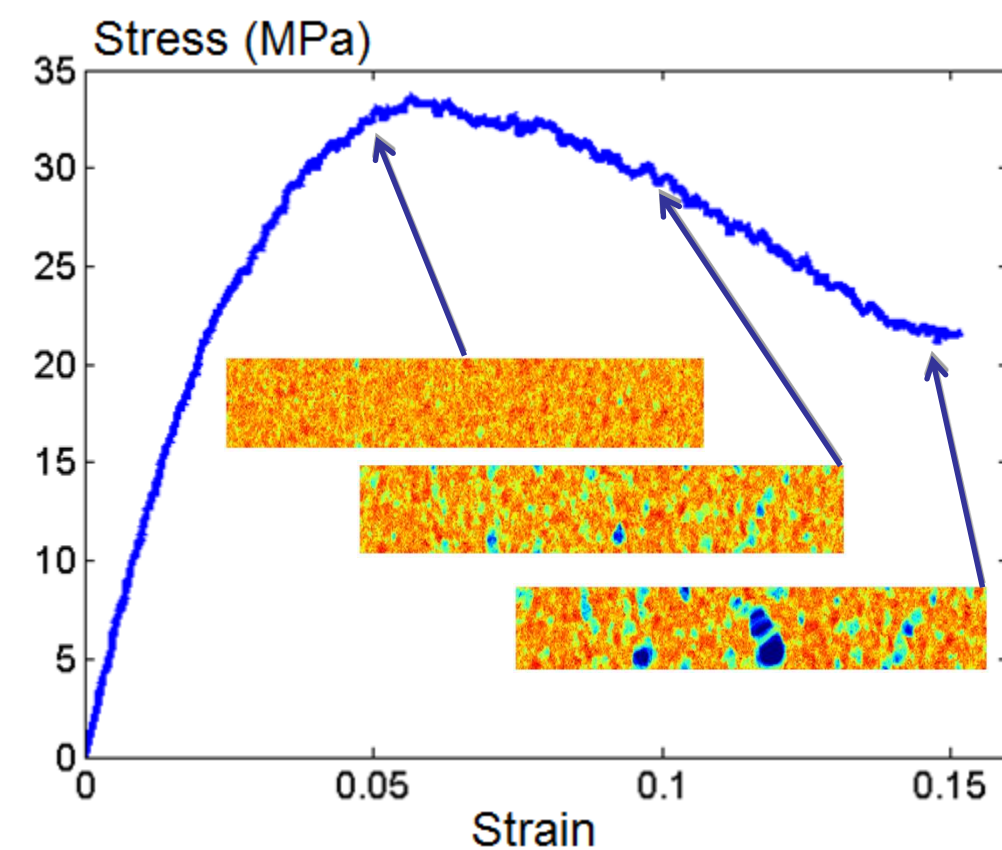


Figure 3. Stress-strain curve for a pure PE.

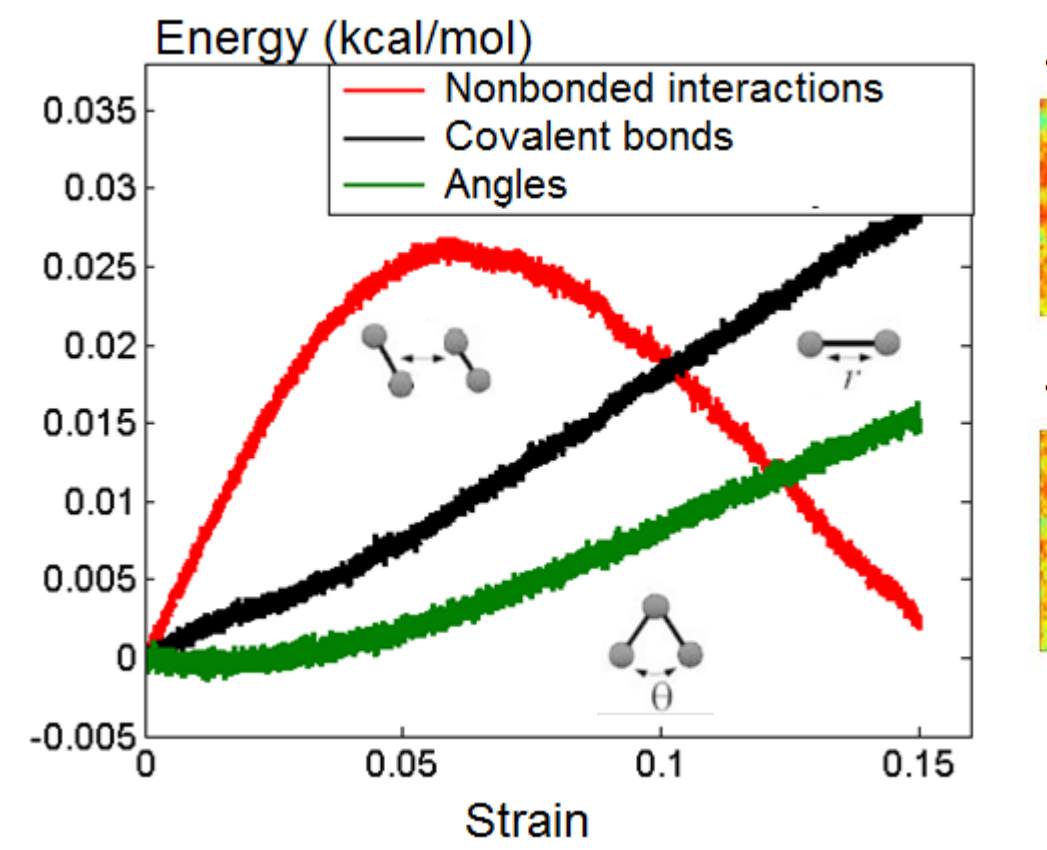


Figure 4. Evolution of different energy components during the deformation.

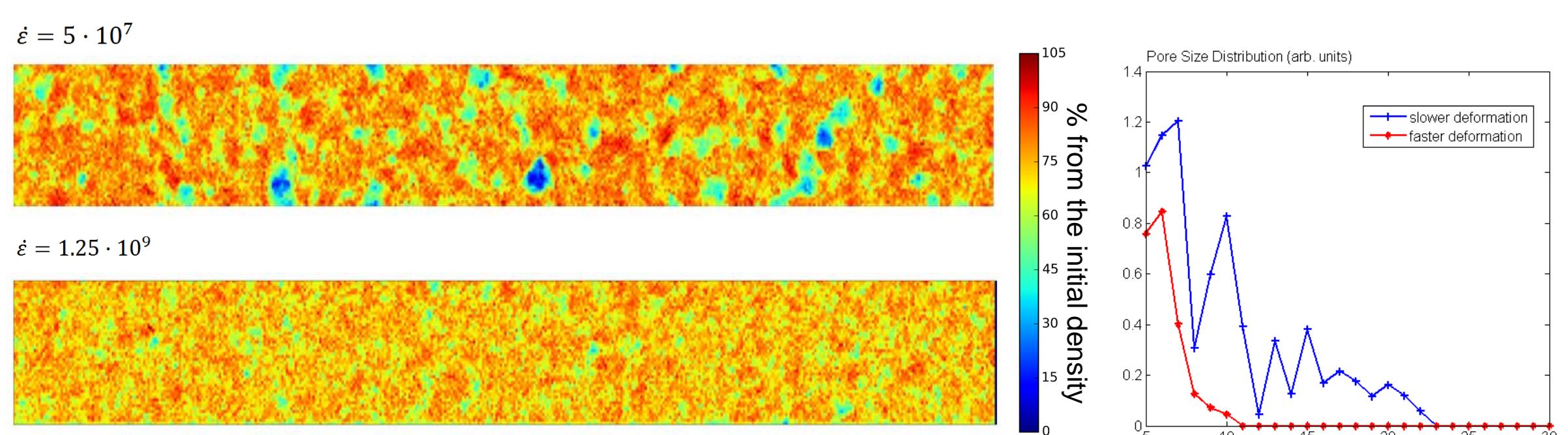
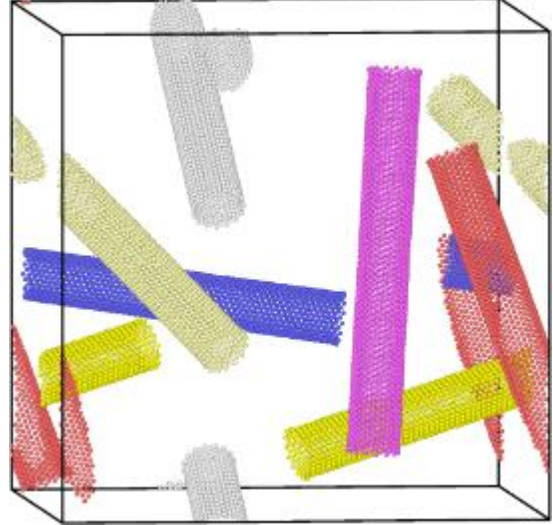


Figure 5. Void nucleation at different deformation rates (density diagram) and corresponding pore size distribution.

Analysis of deformation behavior of the nanocomposite

13 nm long CNTs



In this section the analysis of two types of nanocomposite: the pure PE and PE with CNTs is discussed. The size of simulation cells was 20x20x20 nm³. The first one contained 560 PE chains and 6 CNTs with a length of 13 nm and a diameter of 2 nm. The position of carbon nanotubes is shown in Figure 6. The second contained 560 PE chains with 24 CNTs with a length of 3 nm (Figure 7).

Figure 6. Position of nanotubes in simulation cell 20x20x20 nm³

3 nm long CNTs

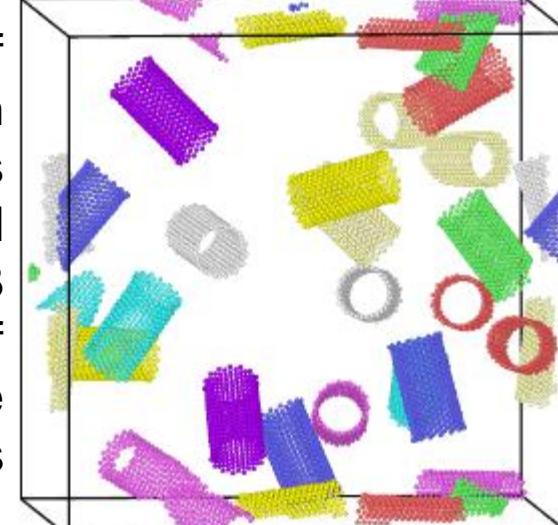


Figure 7. Position of nanotubes in simulation cell 20x20x20 nm³

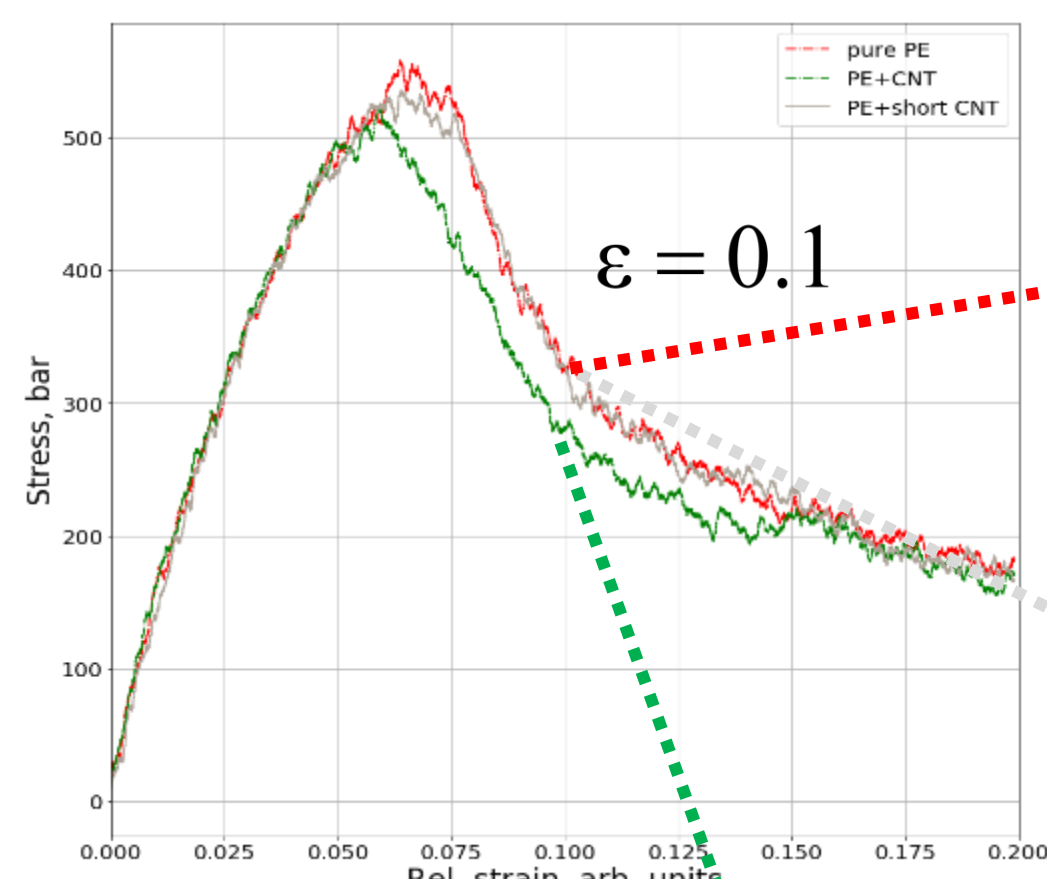


Figure 8. Stress-strain curves of pure PE and PE with CNTs

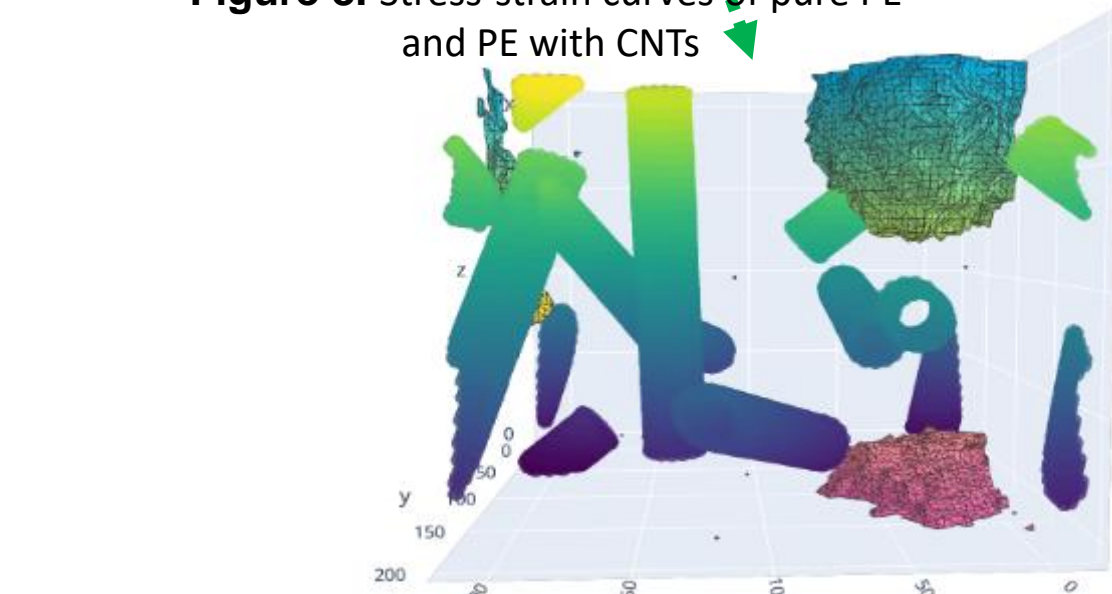


Figure 9. Pores distribution for PE with 13 nm CNTs

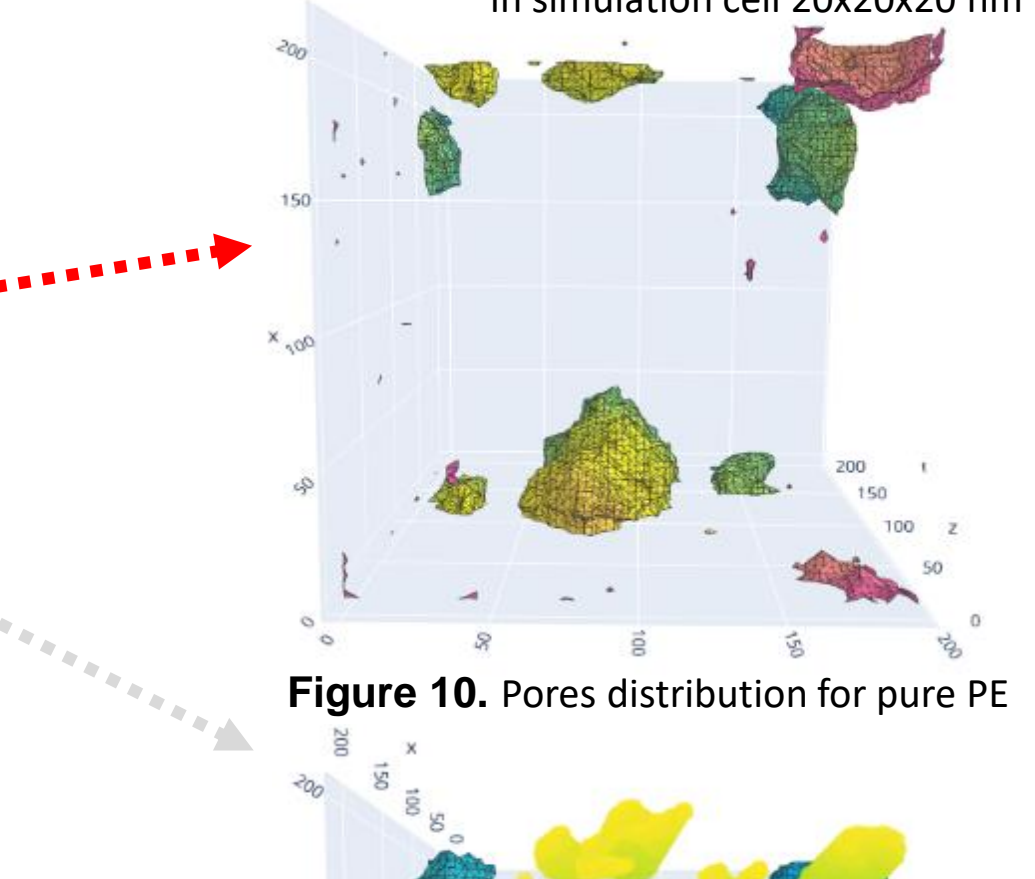


Figure 10. Pores distribution for pure PE

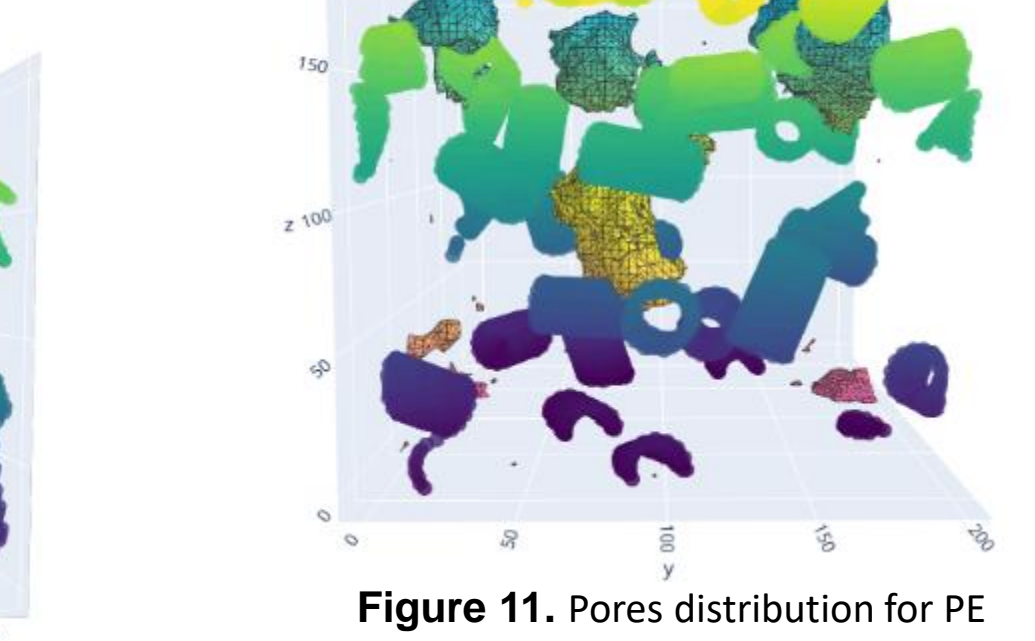


Figure 11. Pores distribution for PE with 3 nm CNTs

Uniaxial deformation along Ox axis with P_{yy} = 0, P_{zz} = 0

In this section the deformation process was performed via uniaxial stretching along OX axis of the computational cell with a condition P_{yy} = 0, P_{zz} = 0 for stress along OY and OZ directions. The deformation was performed at a constant engineering strain rate $\dot{\epsilon} = 1.25 \cdot 10^7 \text{ s}^{-1}$. The kinks in primitive path can be divided in two groups: between polyethylene molecules (PE-PE) and between nanoparticles and polyethylene molecules (NP-PE).

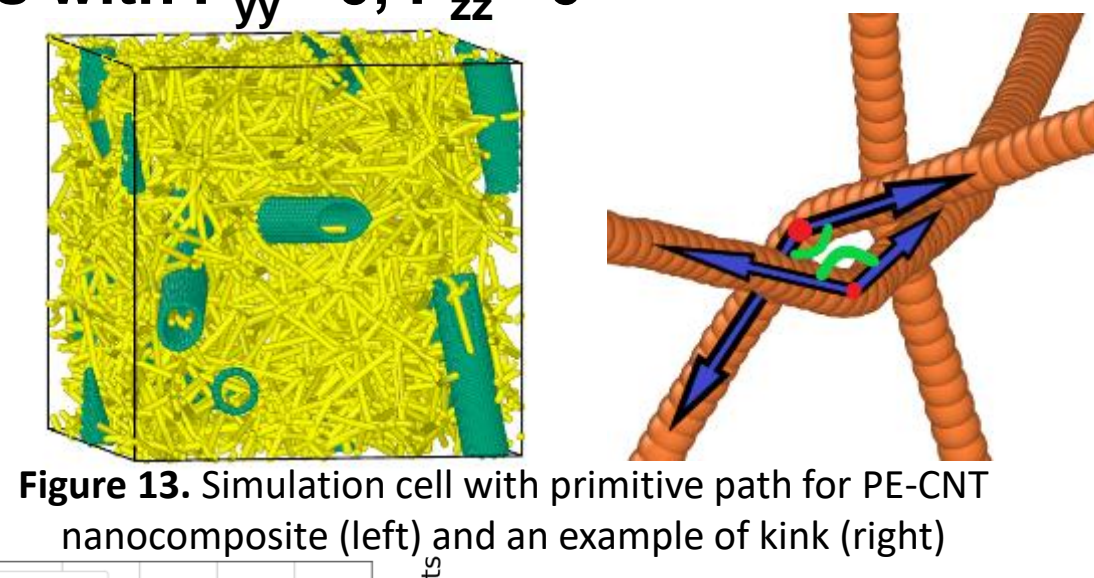


Figure 13. Simulation cell with primitive path for PE-CNT nanocomposite (left) and an example of kink (right)

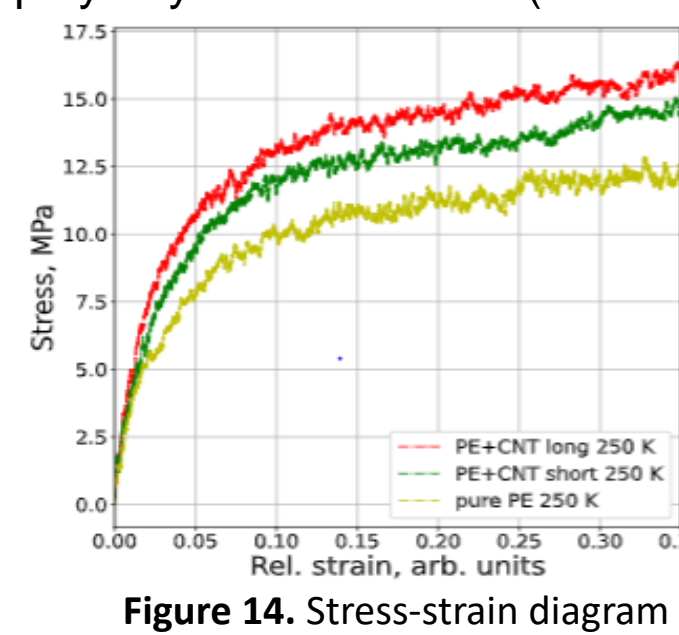


Figure 14. Stress-strain diagram

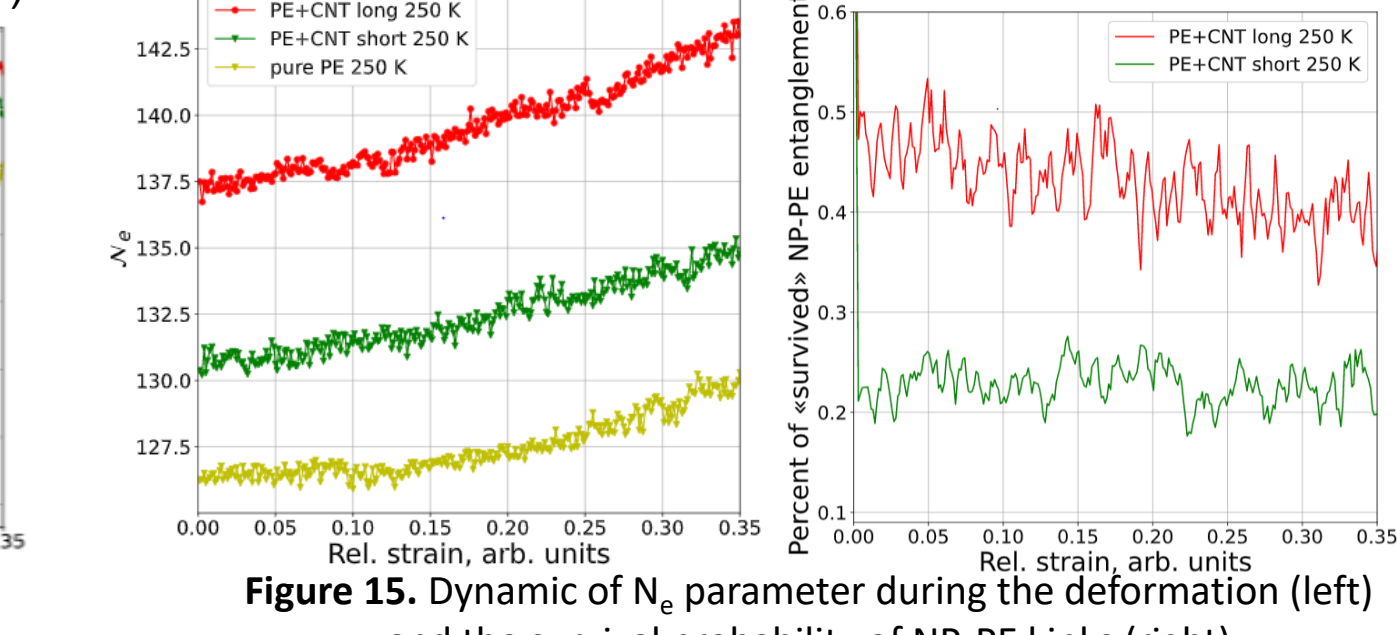


Figure 15. Dynamic of N_e parameter during the deformation (left) and the survival probability of NP-PE kinks (right)

Primitive Path Analysis

Polymer chains system Primitive path network of polymer chains

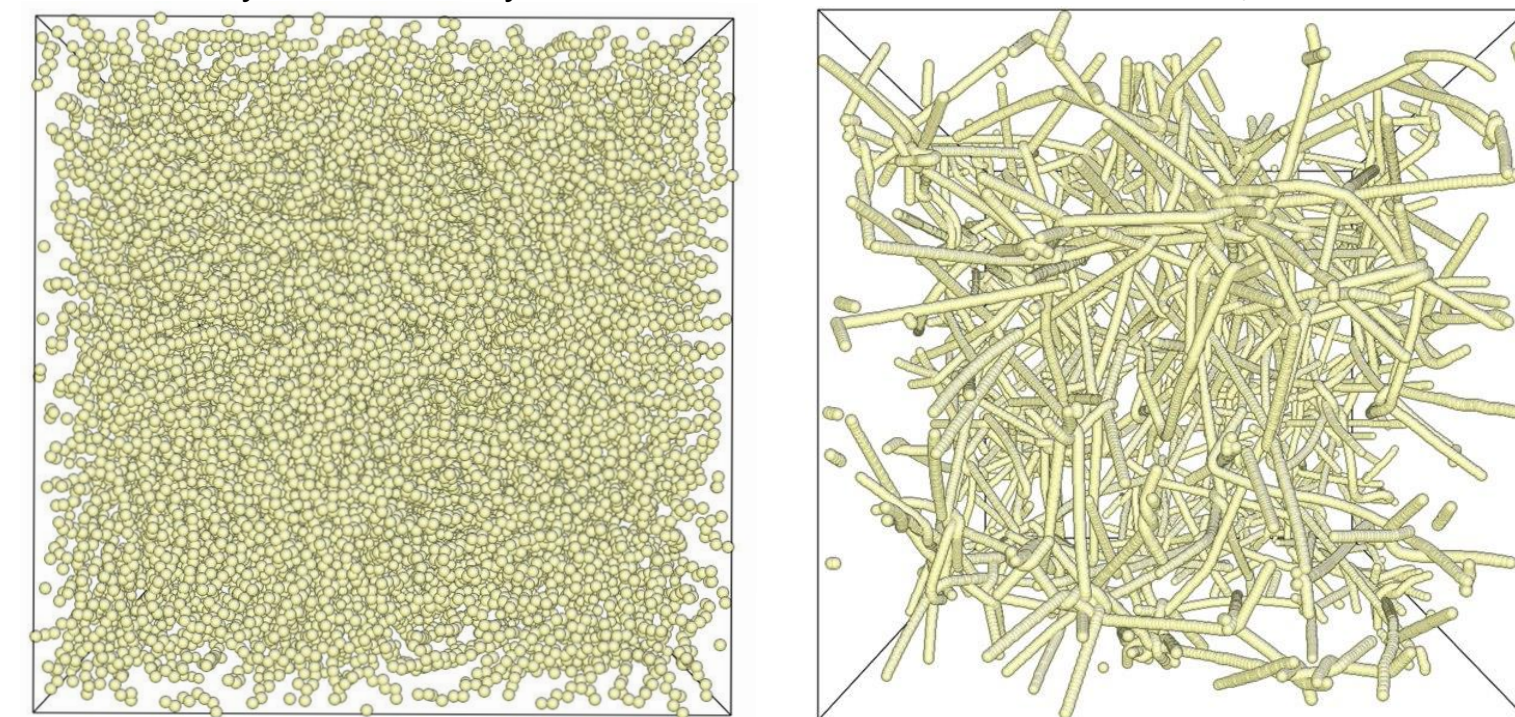


Figure 17. System of polymer chains in two interpretations - the original system and PP network of it.

There is no distinction between polymer-particle and polymer-polymer contacts. When we have information about the number of internal kinks, we can calculate Ne using Ne(contact), where N is the number of beads of the parent chain. If not we will have an alternative way by considering the primitive path as Gaussian chains and measuring the mean squared end-to-end distance (Ree) and the mean contour length (Lpp) of the PP.

$$N_e^{\text{contact}} = \frac{(N-1)N}{Z(N-1)+N} \quad N_e^{\text{statistical}} = (N-1) \frac{R_{ee}^2}{L_{pp}^2}$$

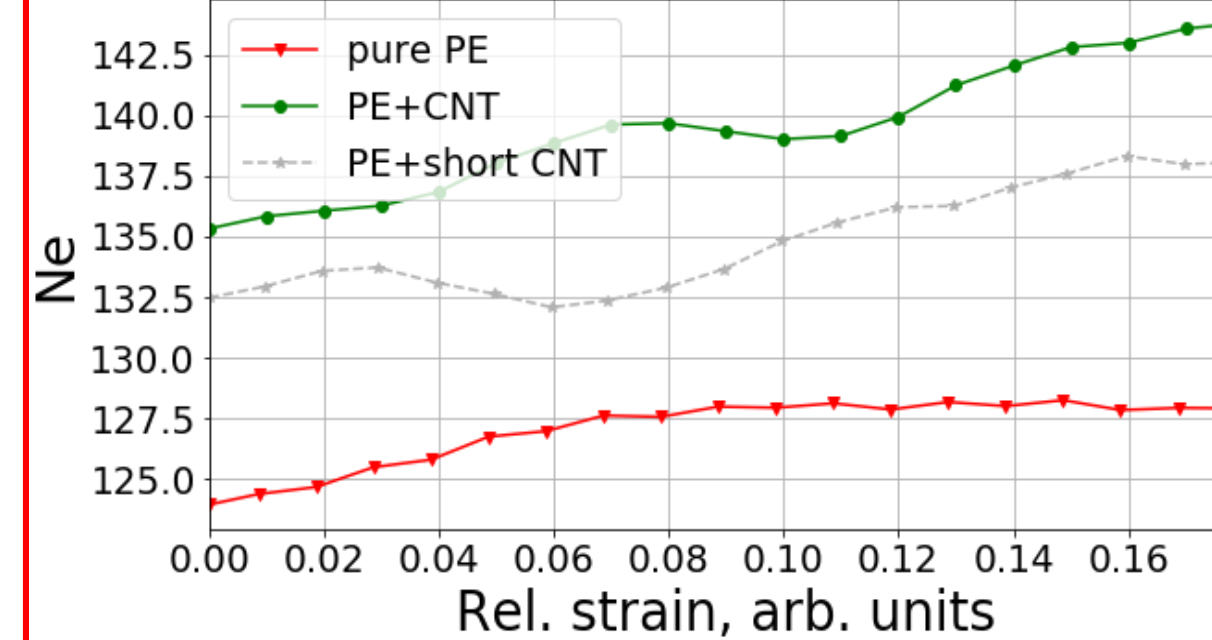


Figure 18. Dependencies of N_e from strain for pure PE and PE with CNTs

Analysis of results for pure PE and PE with CNTs

PP analysis was used in researching the differences between two nanocomposites. Figure 18 shows that average number of atoms between the kinks of PE is growing for all models. The existence of the CNTs in our nanocomposite make the PE matrix more disentangled. Also the longer CNTs are, the more disentangled system is.

Pores volume analysis

During the uniaxial deformation the pores are growing with different rates in different models. The results are represented in Fig. 19. It shows that CNTs speed up the process of the cavitation. At the same time the size of CNTs influence on that process too. Longer CNTs make the cavitation faster than shorter CNTs. Also figures 9-11 give more visual understanding about the pores distribution in the nanocomposites. The big pore can be determined for system with 13 nm CNTs (Fig. 9). However the nanocomposite with 3 nm CNTs and pure PE don't have such a big pores.

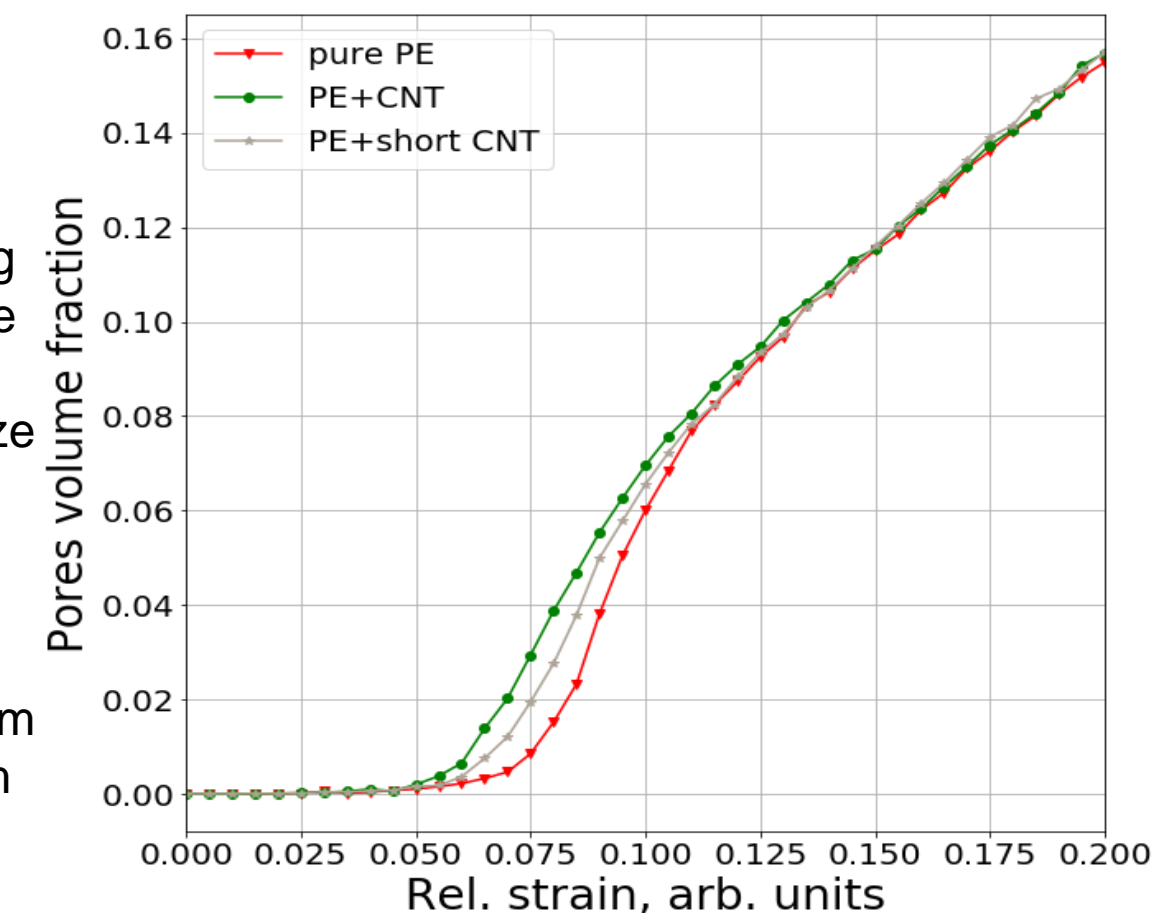


Figure 19. Pores volume growth during the deformation

Conclusions

In the context of primitive path analysis the dependence between the process of chain disentanglement and generation of cavities during the tensile deformation of the system was studied. During the slower deformation we observed more acts of disentanglement and there are generated more nanopores than during faster deformation. Analysis of cavitation in PE-CNT composite during deformation revealed significant impact of nanoparticles on the size distribution of pores. Edges of nanoparticles behaves as inhomogeneities on which pore nucleation starts. In case of high concentration of small CNTs it leads to degradation of elastic properties. Statistical analysis of entanglement lifetimes shows that increasing length of CNTs enhances the stability of nanoparticle-polymer entanglements. It means that visco-elastic properties of the interface layer between polymer matrix and nano-inclusion could differ from those of pure polymer matrix not only due to the difference in the concentration of entanglements, but also due to their higher stability.